V. Low- and High-Mass Protostars and their Environment

https://doi.org/10.1017/S007418090006188X Published online by Cambridge University Press

THE EVOLUTION OF FLOWS AND PROTOSTARS

PHILIPPE ANDRÉ
CEA Service d'Astrophysique, Centre d'Etudes de Saclay
F-91191 Gif-sur-Yvette Cedex, France

Abstract. In this paper, I summarize the key properties of Class 0 protostars, discuss the observational evidence for a decline of outflow/inflow power with evolutionary stage, point out a possible connection with the initial conditions of fast protostellar collapse, and suggest a new collapse scenario in regions of induced, multiple star formation. The main thesis put forward here is that Class 0 objects have unusually powerful outflows because they accrete at a substantially higher rate than their Class I descendants.

1. Introduction

Despite recent observational and theoretical progress, the initial conditions of star formation and the first phases of protostellar collapse remain poorly understood. The purpose of this paper is to show that studying the evolution of molecular outflows through the embedded phase can shed light on this problem by providing important clues to both the mass-loss and the mass-accretion history of protostars.

1.1. TRACKING YSO EVOLUTION

In order to track protostellar evolution one needs a practical age indicator. The evolutionary indicator advocated here is the circumstellar mass derived from (sub)millimeter continuum measurements (André, Ward-Thompson, & Barsony 1993 – hereafter AWB93; André & Montmerle 1994 – hereafter AM94; Saraceno et al. 1996). Independently of the details of any protostellar theory, and in a statistical sense at least, one expects larger amounts of circumstellar material to surround younger stellar objects. In the case of embedded protostars, this decrease of circumstellar mass with time results

B. Reipurth and C. Bertout (eds.), Herbig–Haro Flows and the Birth of Low Mass Stars, 483–494.

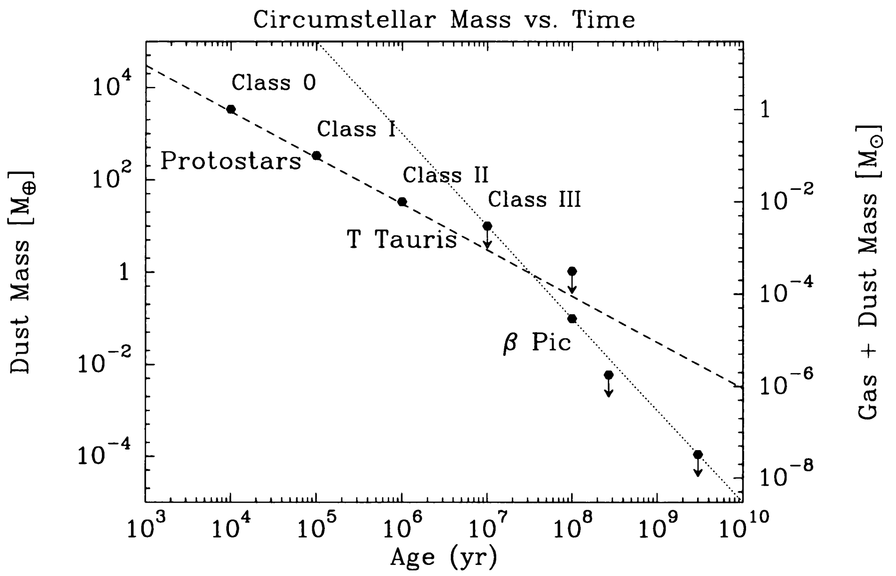

Figure 1. Circumstellar dust mass (in earth masses – left axis) as a function of age for low-mass stars, based on (sub)millimeter continuum measurements by AM94 and Zuckerman & Becklin (1993). The right axis gives estimates of the corresponding total masses (in solar masses), assuming a constant gas-to-dust mass ratio of 100. For comparison, the dashed and dotted lines show t^{-1} and t^{-2} variations of mass with time, respectively.

from the progressive dissipation of the protostellar envelope through accretion and ejection. For instance, in the standard theory of Shu et al. (1987), the mass enclosed within a given radius R of the infalling envelope scales approximately as $M_{env}(r < R) \propto t^{-1/2}$ with time.

The advent of sensitive bolometer arrays on large radiotelescopes such as the IRAM 30 m and the JCMT provides a very effective method of measuring the circumstellar mass around YSOs of any type by mapping their dust continuum emission in the (sub)millimeter range. Thanks to the small dust optical depth at these wavelengths, the measured emission is directly proportional to the circumstellar dust mass. The total (gas + dust) circumstellar mass may be derived if the gas-to-dust ratio is assumed or can be calibrated. The dust absorption coefficient is not exactly known, but the uncertainties are much reduced when the appropriate dust model is used for each type of sources (see Henning, Michel, & Stognienko 1995).
The effectiveness of this time clock is illustrated in Figure 1 which shows a global decline in the median circumstellar mass from protostars to main-

https://doi.org/10.1017/S007418090006188X Published online by Cambridge University Press

sequence stars, going approximately as $(\mathrm{age})^{-1}$ or $(\mathrm{age})^{-2}$. In this figure, the ages of Class 0 and Class I YSOs have been assumed to equal their respective lifetimes as derived from statistical arguments (e.g. AM94), while those of optically visible stars are estimated from positions in the HR diagram.

1.2. DEFINING PROPERTIES OF CLASS 0 PROTOSTARS

Following the above ideas, AWB93 introduced the concept of Class 0 protostars and proposed an age ordering of embedded YSOs based on the submillimeter to bolometric luminosity ratio $\mathrm{L}_{\mathrm{submm}}^{\lambda>350\mu}/\mathrm{L}_{\mathrm{bol}}$. While the (integrated) submillimeter luminosity $L_{submm}^{\lambda>350\mu}$ provides a relative measure of the (total) circumstellar mass $\mathrm{M}_{\mathrm{env}}$, the bolometric luminosity $\mathrm{L}_{\mathrm{bol}}$ may be used to constrain the central stellar mass $M_\star$ (see AM94). In the youngest sources, $\mathrm{L}_{\mathrm{submm}}^{\lambda>350\mu}/\mathrm{L}_{\mathrm{bol}}$ should tend to reproduce the variations of the mass ratio $M_{env}/M_\star$, which is expected to decrease with protostellar age.
AWB93 defined Class 0 sources as those young stellar objects which have $\mathrm{L}_{submm}^{\lambda>350\mu}/\mathrm{L}_{bol} > 5 \times 10^{-3}$. [A roughly equivalent, but more practical, criterion is $\mathrm{S}_{1.3mm}^{int}(d/160pc)^2/L_{\mathrm{bol}} \sim 0.2$ Jy/$\mathrm{L}_\odot$.]
Since such sources are often undetected shortward of 10 μm, the existence of the central YSO is only indirectly inferred from, e.g., the detection of compact VLA radio continuum emission (e.g. Bontemps et al. 1995), or the presence of a collimated CO outflow (see Bachiller 1996). The formal $\mathrm{L}_{submm}^{\lambda>350\mu}/\mathrm{L}_{bol}$ boundary given above between Class 0 YSOs and the more evolved Class I sources of Lada (1987) was set so as to correspond to a mass ratio $M_{env}/M_\star = 1$, assuming the most plausible relations between L_{bol} and $M_\star$ on the one hand and between $\mathrm{L}_{\mathrm{submm}}^{\lambda>350\mu}$ and M_{env} on the other hand (see AWB93 and AM94 for details). *Class 0 sources are thus excellent candidates for being very young protostars in which a hydrostatic core has already formed but not yet accreted the bulk of its final mass.* As most of their mass is still in the form of a dense circumstellar envelope, Class 0 objects can potentially tell us a lot about the physics of protostellar collapse.

2. Evidence for a Decline of Outflow/Inflow Power with Time

Class 0 protostars tend to drive powerful, "jet–like" CO molecular outflows (see review by Bachiller 1996). In contrast, the CO outflows from Class I sources tend to be poorly collimated and much less powerful.

In an effort to quantify this evolution of molecular outflows during the protostellar phase, Bontemps et al. (1996 – hereafter BATC) have obtained and analyzed a homogeneous set of CO(2–1) data around a large sample of low-luminosity ($L_{bol} < 50$ $L_\odot$), nearby ($d < 450$ pc) embedded YSOs,

https://doi.org/10.1017/S007418090006188X Published online by Cambridge University Press

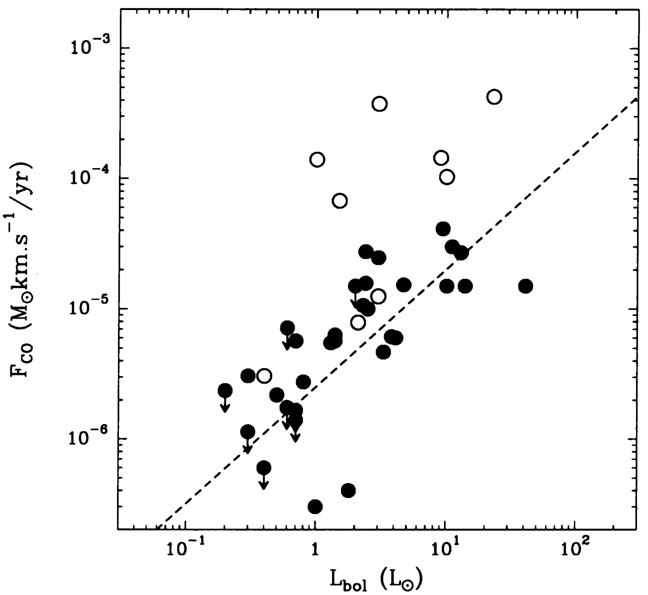

Figure 2. CO momentum flux versus bolometric luminosity for a sample of Class 0 (open circles) and Class I (filled circles) sources. The 'best fit' F_{CO}–L_{bol} correlation found for Class I sources is plotted as a dashed line. Taken from Bontemps et al. (1996).

including 36 Class I sources and 9 Class 0 sources. The results of these observations show that essentially *all* embedded YSOs have some degree of outflow activity, suggesting the outflow phase and the infall/accretion phase coincide. This is consistent with the idea that accretion cannot proceed without ejection and that outflows are directly powered by accretion (e.g. Pudritz et al. 1991, Shu et al. 1994, Ferreira & Pelletier 1995).

More importantly, in the F_{CO}–L_{bol} diagram shown in Figure 2, Class 0 objects lie an order of magnitude above the well-known correlation between outflow momentum flux (F_{CO}) and bolometric luminosity (L_{bol}) that holds for Class I sources. Since lower projected velocities, and thus lower apparent momentum fluxes, are expected from outflows more inclined to the line of sight, this indicates that Class 0 objects are not merely highly obscured Class I sources viewed edge-on: Class 0 objects differ qualitatively from Class I sources *independently of inclination effects.*

Furthermore, BATC find that outflow momentum flux is well correlated with circumstellar envelope mass in their *entire* sample (which includes both Class I and Class 0 sources). Bontemps et al. argue that this new correlation is independent of the F_{CO}–L_{bol} correlation and most likely results from a progressive decrease of outflow power with time during the accretion phase.

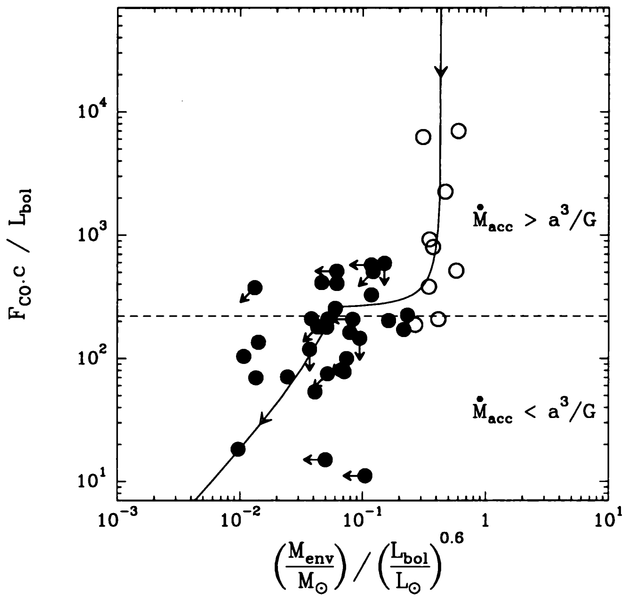

Figure 3. $F_{CO}\,c/L_{bol}$ versus $M_{env}/L_{bol}{}^{0.6}$ for the sample of Class 0 (open circles) and Class I (filled circles) sources studied by Bontemps et al. (1996). The normalized momentum flux $F_{CO}\,c/L_{bol}$ can be taken as an empirical tracer of the accretion rate $\dot{M}_{acc}$ providing there is no significant luminosity evolution (see § 2.1); $M_{env}/L_{bol}{}^{0.6}$ is an evolutionary indicator which decreases with time (see § 1). This diagram should therefore mainly reflect the evolution of $\dot{M}_{acc}$ during the embedded phase. The solid curve shows the accretion rate history predicted by the model of Henriksen et al. (1997) (see § 4).

This is illustrated in the $F_{CO}\,c/L_{bol}$ versus $M_{env}/L_{bol}{}^{0.6}$ diagram of Figure 3, which should be essentially free of any luminosity effect.

2.1. INTERPRETATION OF THE OBSERVED OUTFLOW EVOLUTION

Since magneto-centrifugal accretion/ejection models of bipolar outflows (e.g. Shu et al. 1994, Ferreira & Pelletier 1995) predict that the mass-loss rate is a definite fraction of the mass-accretion rate (typically, $\dot{M}_{jet} \sim 0.1\,\dot{M}_{acc}$), BATC suggest that the decline of outflow power with evolutionary stage seen in Figure 3 reflects a corresponding decrease in the mass-accretion/infall rate.

In the picture of accretion-driven jets/outflows, the CO outflow momentum flux F_{CO} is related to the accretion rate $\dot{M}_{acc}$ by

$$F_{CO} = f_{ent}\,\dot{P}_{jet} = [f_{ent}\,(\dot{M}_{jet}/\dot{M}_{acc})\,V_{jet}] \times \dot{M}_{acc},$$

where $f_{\rm ent}$ is the efficiency of entrainment of the flow by the jet, $\dot{M}_{\rm jet}$ is the mass-loss rate associated with the jet, and $V_{\rm jet}$ is the jet velocity. Using typical values ($f_{\rm ent} \sim 1$, $\dot{M}_{\rm jet}/\dot{M}_{\rm acc} \sim 0.1$, $V_{\rm jet} \sim 100\,{\rm km\,s^{-1}}$), the results of BATC suggest that, *on average*, $\dot{M}_{\rm acc}$ declines from $\sim 10^{-5}\,{\rm M_\odot yr^{-1}}$ for the youngest Class 0 protostars to $\sim 2\times10^{-7}\,{\rm M_\odot yr^{-1}}$ for the most evolved Class I sources, corresponding to a decrease of $\dot{M}_{\rm jet}$ from $\sim 10^{-6}\,{\rm M_\odot yr^{-1}}$ to $\sim 2\times10^{-8}\,{\rm M_\odot yr^{-1}}$. Note, however, that Ophiuchus YSOs and Taurus YSOs seem to follow quite different accretion/ejection histories (see § 4.2, Fig. 6, and Fig. 7 below).

3. Link to the Initial Conditions of Star Formation

As shown by Henriksen (1994), the beginning of the accretion phase depends quite critically on the initial conditions of fast protostellar collapse. In the standard theory of low-mass star formation, the initial conditions correspond to singular isothermal spheres (SISs), which have $\rho_{SIS}(r) = (a^2/2\pi G)r^{-2}$ where a is the isothermal sound speed. This leads to a constant accretion rate $\dot{M}_{\rm acc} \sim a^3/G$ (Shu 1977), which is apparently in conflict with the conclusions of § 2 above. Now, the SIS is obviously an idealized model of the actual pre-collapse conditions. Recent results suggest that, in the real world, the initial conditions differ sometimes significantly from a singular isothermal sphere.

In particular, submillimetre dust continuum mapping shows that the radial density profiles of isolated pre-stellar cores are relatively steep towards their edges (i.e., sometimes steeper than $\rho(r) \propto r^{-2}$), but *flatten out* near their centers, becoming less steep than $\rho(r) \propto r^{-2}$ (Ward-Thompson et al. 1994; André, Ward-Thompson, & Motte 1996 – AWM96). A representative, well-documented example of an isolated pre-stellar core is provided by L1689B, which is located in the ρ Ophiuchi complex but outside the main cloud. In this case, the radial density profile approaches $\rho(r) \propto r^{-2}$ between $\sim$ 4000 AU and $\sim$ 15000 AU, and is as flat as $\rho(r) \propto r^{-0.4}$ or $\rho(r) \propto r^{-1.2}$ (depending on the deprojection hypothesis) at radii less than $\sim$ 4000 AU (see AWM96 and Fig. 4).
By contrast, *protostellar* envelopes are always found to be strongly centrally peaked and do *not* exhibit the inner flattening seen in *pre-stellar* cores (Ladd et al. 1991, Motte et al. 1996).

Fragmentation introduces an additional complication in regions of multiple star formation. For instance, the ρ Ophiuchi main cloud is a star-forming cluster where the fragmentation size scale is clearly much smaller than 0.1 pc (e.g. Motte et al. 1997). In this case, the radius of the 'sphere of influence' of any given protostar must be less than $\sim$ 4000 AU, and the scale-free approximation associated with the SIS must quickly break down.

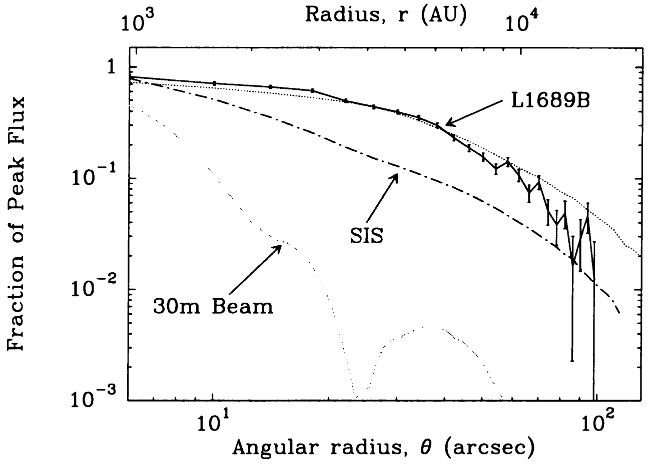

Figure 4. Azimuthally averaged intensity profile of the pre-stellar core L1689B (solid line), as observed with the IRAM 30 m telescope at 1.3 mm (adapted from AWM96). For comparison, the dash-dotted curve shows a spherically symmetric, isothermal model with $\rho(r) \propto r^{-2}$ such as a SIS. The dotted curve represents a spherical model with $\rho(r) \propto r^{-1.3}$ for $r < 4000$ AU (i.e., $\theta < 25''$) and $\rho(r) \propto r^{-2}$ for $r \geq 4000$ AU. The telescope beam profile is shown as a light dotted curve. The model profiles result from a full simulation of the continuum dual-beam mapping technique (see Motte et al. 1996).

Interestingly, recent large-scale, high-angular resolution imaging with the mid-infrared camera on board the ISO satellite (Abergel et al. 1996) suggests that the ρ Oph dense cores are characterized by very sharp edges (i.e., steeper than $\rho \propto r^{-3}$ or $\rho \propto r^{-4}$), possibly produced by external pressure. (The ρ Oph cores are seen as deep absorption structures by ISOCAM.)

4. Suggested Collapse Scenario

In order to improve our understanding of the accretion phase history in the case of non-singular initial conditions, Henriksen, André, & Bontemps (1997 – hereafter HAB97) have recently carried out simplified, analytical calculations of protostellar collapse based on the following assumptions. The initial conditions are represented by an idealized pre-stellar core which consists of a strictly flat inner plateau up to a radius r_N, an r^{-2} 'envelope' up to r_B, and a steeper power-law 'environment' farther out (see Fig. 5). The core collapse is initiated by an external disturbance at $t = t_o < 0$. It is supposed that, after a transitional period (leading to, e.g., magnetic decoupling), supersonic velocities develop *prior to* stellar core formation. The flat inner core region is then free to collapse, essentially homologously due to

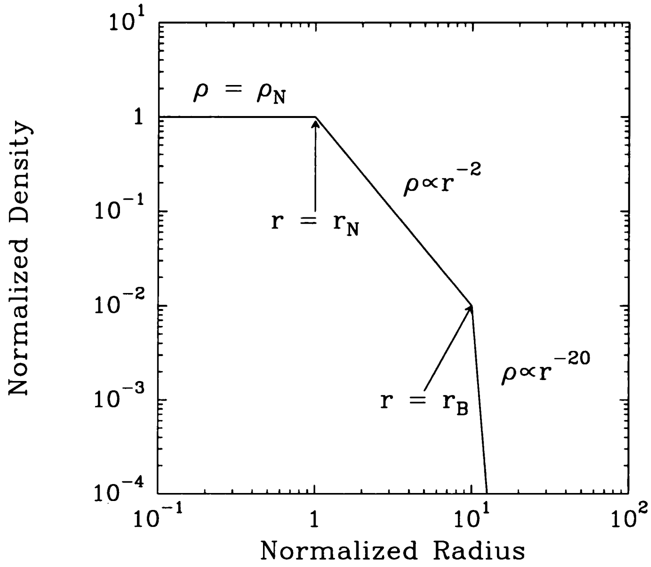

Figure 5. Density *vs.* radius in log–log format for an idealized pre-stellar core corresponding to the initial conditions of the collapse model proposed by HAB97.

the absence of significant pressure gradients. In this case, pressure-free calculations are justified and give qualitatively correct answers, as confirmed by comparison with recent numerical computations which fully account for pressure effects (Foster & Chevalier 1993, Tomisaka 1996). In the calculations of HAB97, the beginning of free core collapse is taken to be at $t = t_1 \equiv -t_{ff}(N)$. The core collapse is thus complete at $t = 0$, where $t_{ff}(N)$ is the free-fall time of a uniform sphere from rest. For all times $t > t_1$, the evolution is assumed to be of the 'gravity-dominated' self-similar form (see HAB97 for details), given uniquely by the density profile at the $t = t_1$ epoch.

In this scenario, the collapse occurs in various stages. The first stage ($t_1 < t < 0$) corresponds to the nearly isothermal, dynamical collapse of the pre-stellar flat inner region, which ends with the formation of a *finite-mass* stellar nucleus. At this stage, the flow is characterized by an inward-going compression wave (see Whitworth & Summers 1985). Observationally, this initial phase, which does not exist in the standard Shu picture, should correspond to 'isothermal protostars', i.e., supersonically collapsing cloud fragments with no central YSOs (see Mezger et al. 1992). It is followed at $t > 0$ by the main accretion/ejection phase, during which the non-zero central point mass accretes the surrounding envelope. The evolution can then be described by an inside-out expansion wave reminiscent of the standard Shu (1977) solution. However, because of the significant infall velocity field achieved during the first collapse stage, the accretion rate is initially higher than in the Shu theory. Enhanced accretion persists as long as the gravitational pull of the initial point mass remains significant. The accretion rate then quickly converges towards the characteristic value $\sim a^3/G$, which is the constant rate found by Shu (1977). At late times, accretion of the outer environment leads to a terminal phase of residual accretion/ejection, during which the accretion rate declines below the Shu value.

When the boundary radius r_B is not much larger than the radius r_N of the flat inner plateau (i.e. $r_B \sim 1.6\, r_N$), the simplified model of HAB97 provides a good overall fit of the diagram of outflow efficiency $F_{\rm CO}\, c/L_{\rm bol}$ versus normalized envelope mass $M_{\rm env}/{L_{\rm bol}}^{0.6}$ observed by BATC (see Figure 3 above). This requires that the fraction of cloud mass in the central plateau region be relatively large, $M_N/M_{cloud} \sim 30$ %.

Based on the fit shown in Figure 3, HAB97 tentatively associate the short initial period of energetic accretion/ejection predicted by their model at the beginning of the accretion phase with the observationally-defined Class 0 stage (AWB93, see § 1.2). In this view, Class I objects are more evolved and correspond to the longer period of moderate accretion/ejection when the accretion rate approaches the Shu value ($\dot{M}_{\rm acc} \lesssim a^3/G$).

4.1. ACCRETION LUMINOSITIES OF CLASS 0 AND CLASS I SOURCES

If, as proposed by BATC and HAB96, $\dot{M}_{\rm acc}$ is a factor of ~ 10 larger for Class 0 sources than for Class I sources, one may naively expect the former to have much higher accretion luminosities than the latter. This would be in apparent contradiction with observations which indicate that Class 0s are not significantly over-luminous compared to Class Is. For instance, in the embedded YSO sample of BATC, the ratio of the average bolometric luminosities for the two classes is $< L_{\rm bol} >_0 / < L_{\rm bol} >_I \sim 1.6$.

In reality, several factors contribute to reduce the theoretical accretion luminosity ($L_{acc} = GM_\star \dot{M}_{acc}/R_\star$) at the Class 0 stage:

(1) The central stellar mass $M_\star$ is smaller for Class 0 sources;

(2) The stellar radius $R_\star$ is likely to be larger if $\dot{M}_{\rm acc}$ is higher, since one expects the rough scaling $R_\star \propto {\dot{M}_{\rm acc}}^{1/3}$ (see Fig. 7 of Stahler 1988);

(3) The amount of accretion energy dissipated in the wind can be expected to be larger for Class 0s than for Class Is (and could be a significant fraction of the total accretion energy).

As shown in HAB97, the combined effects of (1), (2), (3) above are likely to render the luminosities of Class 0 sources similar to those of Class I.

https://doi.org/10.1017/S007418090006188X Published online by Cambridge University Press

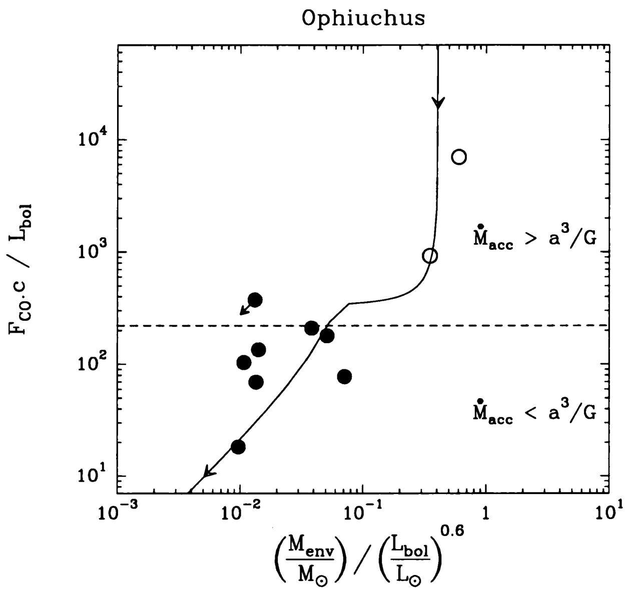

Figure 6. Same $F_{CO}\,c/L_{bol}$ versus $M_{env}/L_{bol}{}^{0.6}$ diagram as Fig. 3, but for the sub-sample of Class 0 (open circles) and Class I (filled circles) sources observed by BATC in Ophiuchus. The solid curve shows the model accretion history advocated by HAB97 (see text).

4.2. DIFFERENCES BETWEEN OPHIUCHUS AND TAURUS

In ρ Ophiuchi, the model fit of Figure 6 suggests that the Class 0 sources are in the initial phase of vigorous accretion with $\dot{M}_{acc} \sim 10^{-4}\,M_\odot yr^{-1}$, while the Class I sources may be in their terminal accretion phase with $\dot{M}_{acc} \lesssim 10^{-5}\,M_\odot yr^{-1}$. The latter is not surprising since, due to the small fragmentation size scale in this cloud (e.g. Motte et al. 1997), the expansion wave characterizing the collapse at $t > 0$ will reach the boundary of any given protostellar envelope/core in a time $t_B = r_B/a \lesssim 5\times10^4$ yr (assuming $a = 0.35\,\mathrm{km\ s^{-1}}$), shorter than the typical Class I lifetime of $\sim 2\times10^5$ yr (estimated by, e.g., Greene et al. 1994).
The clear contrast seen in Figure 6 between Class 0 and Class I objects strongly supports the contention that, in star-forming clusters at least, these two classes of YSOs differ qualitatively (AWB93).

On the other hand, all the Taurus sources of Figure 7 appear to be in the 'asymptotic' phase during which the accretion rate is approximately that predicted by the Shu theory, i.e., $\dot{M}_{acc} \sim a^3/G \sim 2\times10^{-6}\,M_\odot yr^{-1}$ (see also Kenyon, Calvet, & Hartmann 1993). In this case there is a much

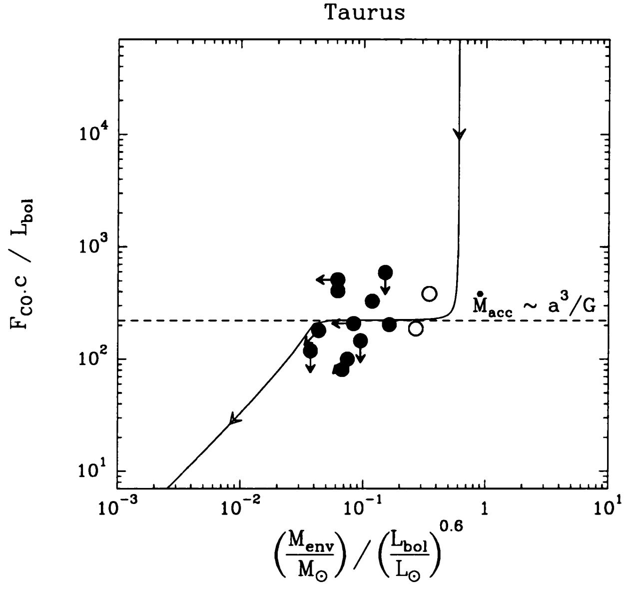

Figure 7. Same as Fig. 6 but for the sub-sample of candidate Class 0 (open circles) and Class I (filled circles) protostars observed by BATC in Taurus.

better continuity between the two classes, suggesting the candidate Class 0 protostars of Taurus may be viewed as "extreme Class I" sources.

5. Conclusions

Measuring outflow strength as a function of envelope mass in large, representative samples of embedded YSOs is a powerful, albeit indirect, tool to gain insight into the mass-accretion history of protostars.

Our recent work (BATC and HAB97) suggests that the protostellar accretion rate is roughly constant in Taurus, in agreement with the $\sim a^3/G$ value predicted by the 'standard' theory of Shu and collaborators. This is consistent with the idea that most Taurus stars form in relative isolation, following the *self-initiated* contraction/collapse of dense cores due to ambipolar diffusion (e.g. Mouschovias 1991). The initial conditions of fast protostellar collapse are then effectively close to a singular isothermal sphere (e.g. Li & Shu 1996).

However, our results also suggest that Class 0 protostars in star-forming clusters such as ρ Ophiuchi accrete at a significantly higher rate than the standard a^3/G value, and much more vigorously than their Class I descendants. In our view, this is because, in these regions, star formation is *induced* by the impact of (slow) shock waves (e.g. Loren & Wootten 1986, Boss 1995), and the collapse initial conditions depart significantly from a singular isothermal sphere. In this case, the collapse scenario proposed by HAB97 (see § 4), which predicts a strong decline of the accretion rate at the beginning of the main accretion phase, is likely to provide a better description of early protostellar evolution than the standard theory.

Acknowledgements: It is a pleasure to thank my colleagues S. Bontemps, R. Henriksen, F. Motte, and D. Ward-Thompson for their contributions to the work presented in this paper.

References

Abergel, A., Bernard, J.P., Boulanger, F. et al. 1996, A&A, 315, L329
André, P., Montmerle, T. 1994, ApJ 420,837 – AM94
André P., Ward-Thompson D., Barsony M., 1993, ApJ, 406, 122 – AWB93
André P., Ward-Thompson D., Motte, F. 1996, A&A, 314, 625 – AWM96
Bachiller, R. 1996, A.R.A.A., 34, 111
Bontemps, S., André, P., & Ward-Thompson, D. 1995, A&A, 297, 98
Bontemps, S., André, P., Terebey, S. & Cabrit, S. 1996, A&A, 311, 858 – BATC
Boss, A.P. 1995, ApJ 439, 224
Ferreira, J., Pelletier, G. 1995, A&A 295,807
Foster, P.N., Chevalier, R.A. 1993, ApJ 416,303 – FC93
Greene T.P., Wilking B.A., André P., Young E.T., Lada C.J. 1994, ApJ 434, 614
Henning, Th., Michel, B., & Stognienko, R. 1995, Planet. Space Sci., 43, 1333
Henriksen, R.N. 1994, in: Montmerle T., Lada C.J., Mirabel I.F., Trân Thanh Vân J. (eds.) The Cold Universe. Editions Frontières, p.241 – H94
Henriksen, R.N., André, P., & Bontemps, S. 1997, A&A, in press
Kenyon, S.J., Calvet, N., & Hartmann, L. 1993, ApJ 414, 676
Lada, C.J. 1987, in: Peimbert M., Jugaku J. (eds.) Star Forming Regions. IAU 115, p.1
Ladd, E.F., Adams, F.C., Casey, S. et al. 1991, ApJ 382, 555
Li, S., & Shu, F.H. 1996, ApJ, 472, 211
Loren, R.B., Wootten, A., 1986, ApJ, 306, 142
Mezger, P.G., Sievers, A.W., Haslam, C.G.T., et al. 1992, A&A, 256, 631
Motte, F., André, P., Neri, R. 1996, in: Siebenmorgen, R., Kaufl, H.U. (eds.) The Role of Dust in the Formation of Stars. ESO Astrophysics Symposia. Springer, Berlin, p. 47
Motte, F., André, P., Neri, R. 1997, A&A, in preparation (see Poster Proceedings)
Mouschovias, T.M. 1991, in The Physics of Star Formation and Early Stellar Evolution, Eds. Lada & Kylafis (Kluwer), p. 449
Pudritz, R.E., Pelletier, G, & Gomez de Castro, A.I. 1991, in The Physics of Star Formation and Early Stellar Evolution, Eds. Lada & Kylafis (Kluwer), p. 539
Saraceno P., André P., Ceccarelli C., Griffin M., Molinari S. 1996, A&A, 309, 827
Shu F. 1977, ApJ, 214, 488
Shu, F.H., Adams, F.C., Lizano, S. 1987, ARA&A 25,23
Shu F., Najita J., Ostriker E. et al. 1994, ApJ 429, 781
Stahler S.W. 1988, ApJ 332, 804
Tomisaka, K. 1996, PASJ, 48, L97
Ward-Thompson, D., Scott, P.F., Hills, R.E., & André, P. 1994, MNRAS, 268, 276
Whitworth, A., & Summers, D. 1985, MNRAS, 214, 1
Zuckerman, B., & Becklin, E.E. 1993, ApJ, 414, 793